PHYSICAL REVIEW D **86,** 071701(R) (2012)

Search for $Z\gamma$ events with large missing transverse energy in $p\bar{p}$ collisions at $\sqrt{s} = 1.96$ TeV

V. M. Abazov,[32] B. Abbott,[70] B. S. Acharya,[26] M. Adams,[46] T. Adams,[44] G. D. Alexeev,[32] G. Alkhazov,[36] A. Alton,[58,†]
G. Alverson,[57] M. Aoki,[45] A. Askew,[44] S. Atkins,[55] K. Augsten,[7] C. Avila,[5] F. Badaud,[10] L. Bagby,[45] B. Baldin,[45]
D. V. Bandurin,[44] S. Banerjee,[26] E. Barberis,[57] P. Baringer,[53] J. Barreto,[2] J. F. Bartlett,[45] U. Bassler,[15] V. Bazterra,[46]
A. Bean,[53] M. Begalli,[2] L. Bellantoni,[45] S. B. Beri,[24] G. Bernardi,[14] R. Bernhard,[19] I. Bertram,[39] M. Besançon,[15]
R. Beuselinck,[40] V. A. Bezzubov,[35] P. C. Bhat,[45] S. Bhatia,[60] V. Bhatnagar,[24] G. Blazey,[47] S. Blessing,[44] K. Bloom,[61]
A. Boehnlein,[45] D. Boline,[67] E. E. Boos,[34] G. Borissov,[39] T. Bose,[56] A. Brandt,[73] O. Brandt,[20] R. Brock,[59]
G. Brooijmans,[65] A. Bross,[45] D. Brown,[14] J. Brown,[14] X. B. Bu,[45] M. Buehler,[45] V. Buescher,[21] V. Bunichev,[34]
S. Burdin,[39,‡] C. P. Buszello,[38] E. Camacho-Pérez,[29] B. C. K. Casey,[45] H. Castilla-Valdez,[29] S. Caughron,[59]
S. Chakrabarti,[67] D. Chakraborty,[47] K. M. Chan,[51] A. Chandra,[75] E. Chapon,[15] G. Chen,[53] S. Chevalier-Théry,[15]
D. K. Cho,[72] S. W. Cho,[28] S. Choi,[28] B. Choudhary,[25] S. Cihangir,[45] D. Claes,[61] J. Clutter,[53] M. Cooke,[45] W. E. Cooper,[45]
M. Corcoran,[75] F. Couderc,[15] M.-C. Cousinou,[12] A. Croc,[15] D. Cutts,[72] A. Das,[42] G. Davies,[40] S. J. de Jong,[30,31]
E. De La Cruz-Burelo,[29] F. Déliot,[15] R. Demina,[66] D. Denisov,[45] S. P. Denisov,[35] S. Desai,[45] C. Deterre,[15] K. DeVaughan,[61]
H. T. Diehl,[45] M. Diesburg,[45] P. F. Ding,[41] A. Dominguez,[61] A. Dubey,[25] L. V. Dudko,[34] D. Duggan,[62] A. Duperrin,[12]
S. Dutt,[24] A. Dyshkant,[47] M. Eads,[61] D. Edmunds,[59] J. Ellison,[43] V. D. Elvira,[45] Y. Enari,[14] H. Evans,[49] A. Evdokimov,[68]
V. N. Evdokimov,[35] G. Facini,[57] L. Feng,[47] T. Ferbel,[66] F. Fiedler,[21] F. Filthaut,[30,31] W. Fisher,[59] H. E. Fisk,[45] M. Fortner,[47]
H. Fox,[39] S. Fuess,[45] A. Garcia-Bellido,[66] J. A. García-González,[29] G. A. García-Guerra,[29,§] V. Gavrilov,[33] P. Gay,[10]
W. Geng,[12,59] D. Gerbaudo,[63] C. E. Gerber,[46] Y. Gershtein,[62] G. Ginther,[45,66] G. Golovanov,[32] A. Goussiou,[77]
P. D. Grannis,[67] S. Greder,[16] H. Greenlee,[45] G. Grenier,[17] Ph. Gris,[10] J.-F. Grivaz,[13] A. Grohsjean,[15,∥] S. Grünendahl,[45]
M. W. Grünewald,[27] T. Guillemin,[13] G. Gutierrez,[45] P. Gutierrez,[70] A. Haas,[65,¶] S. Hagopian,[44] J. Haley,[57] L. Han,[4]
K. Harder,[41] A. Harel,[66] J. M. Hauptman,[52] J. Hays,[40] T. Head,[41] T. Hebbeker,[18] D. Hedin,[47] H. Hegab,[71] A. P. Heinson,[43]
U. Heintz,[72] C. Hensel,[20] I. Heredia-De La Cruz,[29] K. Herner,[58] G. Hesketh,[41,**] M. D. Hildreth,[51] R. Hirosky,[76]
T. Hoang,[44] J. D. Hobbs,[67] B. Hoeneisen,[9] M. Hohlfeld,[21] I. Howley,[73] Z. Hubacek,[7,15] V. Hynek,[7] I. Iashvili,[64]
Y. Ilchenko,[74] R. Illingworth,[45] A. S. Ito,[45] S. Jabeen,[72] M. Jaffré,[13] A. Jayasinghe,[70] R. Jesik,[40] K. Johns,[42] E. Johnson,[59]
M. Johnson,[45] A. Jonckheere,[45] P. Jonsson,[40] J. Joshi,[43] A. W. Jung,[45] A. Juste,[37] K. Kaadze,[54] E. Kajfasz,[12]
D. Karmanov,[34] P. A. Kasper,[45] I. Katsanos,[61] R. Kehoe,[74] S. Kermiche,[12] N. Khalatyan,[45] A. Khanov,[71] A. Kharchilava,[64]
Y. N. Kharzheev,[32] I. Kiselevich,[33] J. M. Kohli,[24] A. V. Kozelov,[35] J. Kraus,[60] S. Kulikov,[35] A. Kumar,[64] A. Kupco,[8]
T. Kurča,[17] V. A. Kuzmin,[34] S. Lammers,[49] G. Landsberg,[72] P. Lebrun,[17] H. S. Lee,[28] S. W. Lee,[52] W. M. Lee,[45]
J. Lellouch,[14] H. Li,[11] L. Li,[43] Q. Z. Li,[45] J. K. Lim,[28] D. Lincoln,[45] J. Linnemann,[59] V. V. Lipaev,[35] R. Lipton,[45] H. Liu,[74]
Y. Liu,[4] A. Lobodenko,[36] M. Lokajicek,[8] R. Lopes de Sa,[67] H. J. Lubatti,[77] R. Luna-Garcia,[29,††] A. L. Lyon,[45]
A. K. A. Maciel,[1] R. Madar,[15] R. Magaña-Villalba,[29] S. Malik,[61] V. L. Malyshev,[32] Y. Maravin,[54] J. Martínez-Ortega,[29]
R. McCarthy,[67] C. L. McGivern,[53] M. M. Meijer,[30,31] A. Melnitchouk,[60] D. Menezes,[47] P. G. Mercadante,[3] M. Merkin,[34]
A. Meyer,[18] J. Meyer,[20] F. Miconi,[16] N. K. Mondal,[26] M. Mulhearn,[76] E. Nagy,[12] M. Naimuddin,[25] M. Narain,[72]
R. Nayyar,[42] H. A. Neal,[58] J. P. Negret,[5] P. Neustroev,[36] T. Nunnemann,[22] G. Obrant,[36,*] J. Orduna,[75] N. Osman,[12]
J. Osta,[51] M. Padilla,[43] A. Pal,[73] N. Parashar,[50] V. Parihar,[72] S. K. Park,[28] R. Partridge,[72,¶] N. Parua,[49] A. Patwa,[68]
B. Penning,[45] M. Perfilov,[34] Y. Peters,[41] K. Petridis,[41] G. Petrillo,[66] P. Pétroff,[13] M.-A. Pleier,[68]
P. L. M. Podesta-Lerma,[29,‡‡] V. M. Podstavkov,[45] A. V. Popov,[35] M. Prewitt,[75] D. Price,[49] N. Prokopenko,[35] J. Qian,[58]
A. Quadt,[20] B. Quinn,[60] M. S. Rangel,[1] K. Ranjan,[25] P. N. Ratoff,[39] I. Razumov,[35] P. Renkel,[74] I. Ripp-Baudot,[16]
F. Rizatdinova,[71] M. Rominsky,[45] A. Ross,[39] C. Royon,[15] P. Rubinov,[45] R. Ruchti,[51] G. Sajot,[11] P. Salcido,[47]
A. Sánchez-Hernández,[29] M. P. Sanders,[22] B. Sanghi,[45] A. S. Santos,[1,§§] G. Savage,[45] L. Sawyer,[55] T. Scanlon,[40]
R. D. Schamberger,[67] Y. Scheglov,[36] H. Schellman,[48] S. Schlobohm,[77] C. Schwanenberger,[41] R. Schwienhorst,[59]
J. Sekaric,[53] H. Severini,[70] E. Shabalina,[20] V. Shary,[15] S. Shaw,[59] A. A. Shchukin,[35] R. K. Shivpuri,[25] V. Simak,[7]
P. Skubic,[70] P. Slattery,[66] D. Smirnov,[51] K. J. Smith,[64] G. R. Snow,[61] J. Snow,[69] S. Snyder,[68] S. Söldner-Rembold,[41]
L. Sonnenschein,[18] K. Soustruznik,[6] J. Stark,[11] D. A. Stoyanova,[35] M. Strauss,[70] L. Stutte,[45] L. Suter,[41] P. Svoisky,[70]
M. Takahashi,[41] M. Titov,[15] V. V. Tokmenin,[32] Y.-T. Tsai,[66] K. Tschann-Grimm,[67] D. Tsybychev,[67] B. Tuchming,[15]
C. Tully,[63] L. Uvarov,[36] S. Uvarov,[36] S. Uzunyan,[47] R. Van Kooten,[49] W. M. van Leeuwen,[30] N. Varelas,[46] E. W. Varnes,[42]
I. A. Vasilyev,[35] P. Verdier,[17] A. Y. Verkheev,[32] L. S. Vertogradov,[32] M. Verzocchi,[45] M. Vesterinen,[41] D. Vilanova,[15]
P. Vokac,[7] H. D. Wahl,[44] M. H. L. S. Wang,[45] J. Warchol,[51] G. Watts,[77] M. Wayne,[51] J. Weichert,[21] L. Welty-Rieger,[48]
A. White,[73] D. Wicke,[23] M. R. J. Williams,[39] A. Wilson,[58] G. W. Wilson,[53] M. Wobisch,[55] D. R. Wood,[57] T. R. Wyatt,[41]

1550-7998/2012/86(7)/071701(7)

Y. Xie,[45] R. Yamada,[45] W.-C. Yang,[41] T. Yasuda,[45] Y. A. Yatsunenko,[32] W. Ye,[67] Z. Ye,[45] H. Yin,[45] K. Yip,[68] S. W. Youn,[45] J. Zennamo,[64] T. Zhao,[77] T. G. Zhao,[41] B. Zhou,[58] J. Zhu,[58] M. Zielinski,[66] D. Zieminska,[49] and L. Zivkovic[72]

(D0 Collaboration)

[1]*LAFEX, Centro Brasileiro de Pesquisas Físicas, Rio de Janeiro, Brazil*
[2]*Universidade do Estado do Rio de Janeiro, Rio de Janeiro, Brazil*
[3]*Universidade Federal do ABC, Santo André, Brazil*
[4]*University of Science and Technology of China, Hefei, People's Republic of China*
[5]*Universidad de los Andes, Bogotá, Colombia*
[6]*Charles University, Faculty of Mathematics and Physics, Center for Particle Physics, Prague, Czech Republic*
[7]*Czech Technical University in Prague, Prague, Czech Republic*
[8]*Center for Particle Physics, Institute of Physics, Academy of Sciences of the Czech Republic, Prague, Czech Republic*
[9]*Universidad San Francisco de Quito, Quito, Ecuador*
[10]*LPC, Université Blaise Pascal, CNRS/IN2P3, Clermont, France*
[11]*LPSC, Université Joseph Fourier Grenoble 1, CNRS/IN2P3, Institut National Polytechnique de Grenoble, Grenoble, France*
[12]*CPPM, Aix-Marseille Université, CNRS/IN2P3, Marseille, France*
[13]*LAL, Université Paris-Sud, CNRS/IN2P3, Orsay, France*
[14]*LPNHE, Universités Paris VI and VII, CNRS/IN2P3, Paris, France*
[15]*CEA, Irfu, SPP, Saclay, France*
[16]*IPHC, Université de Strasbourg, CNRS/IN2P3, Strasbourg, France*
[17]*IPNL, Université Lyon 1, CNRS/IN2P3, Villeurbanne, France and Université de Lyon, Lyon, France*
[18]*III. Physikalisches Institut A, RWTH Aachen University, Aachen, Germany*
[19]*Physikalisches Institut, Universität Freiburg, Freiburg, Germany*
[20]*II. Physikalisches Institut, Georg-August-Universität Göttingen, Göttingen, Germany*
[21]*Institut für Physik, Universität Mainz, Mainz, Germany*
[22]*Ludwig-Maximilians-Universität München, München, Germany*
[23]*Fachbereich Physik, Bergische Universität Wuppertal, Wuppertal, Germany*
[24]*Panjab University, Chandigarh, India*
[25]*Delhi University, Delhi, India*
[26]*Tata Institute of Fundamental Research, Mumbai, India*
[27]*University College Dublin, Dublin, Ireland*
[28]*Korea Detector Laboratory, Korea University, Seoul, Korea*
[29]*CINVESTAV, Mexico City, Mexico*
[30]*Nikhef, Science Park, Amsterdam, Netherlands*
[31]*Radboud University Nijmegen, Nijmegen, Netherlands*
[32]*Joint Institute for Nuclear Research, Dubna, Russia*
[33]*Institute for Theoretical and Experimental Physics, Moscow, Russia*
[34]*Moscow State University, Moscow, Russia*
[35]*Institute for High Energy Physics, Protvino, Russia*
[36]*Petersburg Nuclear Physics Institute, St. Petersburg, Russia*
[37]*Institució Catalana de Recerca i Estudis Avançats (ICREA) and Institut de Física d'Altes Energies (IFAE), Barcelona, Spain*
[38]*Uppsala University, Uppsala, Sweden*
[39]*Lancaster University, Lancaster LA1 4YB, United Kingdom*
[40]*Imperial College London, London SW7 2AZ, United Kingdom*
[41]*The University of Manchester, Manchester M13 9PL, United Kingdom*
[42]*University of Arizona, Tucson, Arizona 85721, USA*
[43]*University of California Riverside, Riverside, California 92521, USA*
[44]*Florida State University, Tallahassee, Florida 32306, USA*
[45]*Fermi National Accelerator Laboratory, Batavia, Illinois 60510, USA*
[46]*University of Illinois at Chicago, Chicago, Illinois 60607, USA*
[47]*Northern Illinois University, DeKalb, Illinois 60115, USA*
[48]*Northwestern University, Evanston, Illinois 60208, USA*
[49]*Indiana University, Bloomington, Indiana 47405, USA*
[50]*Purdue University Calumet, Hammond, Indiana 46323, USA*
[51]*University of Notre Dame, Notre Dame, Indiana 46556, USA*
[52]*Iowa State University, Ames, Iowa 50011, USA*
[53]*University of Kansas, Lawrence, Kansas 66045, USA*
[54]*Kansas State University, Manhattan, Kansas 66506, USA*
[55]*Louisiana Tech University, Ruston, Louisiana 71272, USA*

[56]*Boston University, Boston, Massachusetts 02215, USA*
[57]*Northeastern University, Boston, Massachusetts 02115, USA*
[58]*University of Michigan, Ann Arbor, Michigan 48109, USA*
[59]*Michigan State University, East Lansing, Michigan 48824, USA*
[60]*University of Mississippi, University, Mississippi 38677, USA*
[61]*University of Nebraska, Lincoln, Nebraska 68588, USA*
[62]*Rutgers University, Piscataway, New Jersey 08855, USA*
[63]*Princeton University, Princeton, New Jersey 08544, USA*
[64]*State University of New York, Buffalo, New York 14260, USA*
[65]*Columbia University, New York, New York 10027, USA*
[66]*University of Rochester, Rochester, New York 14627, USA*
[67]*State University of New York, Stony Brook, New York 11794, USA*
[68]*Brookhaven National Laboratory, Upton, New York 11973, USA*
[69]*Langston University, Langston, Oklahoma 73050, USA*
[70]*University of Oklahoma, Norman, Oklahoma 73019, USA*
[71]*Oklahoma State University, Stillwater, Oklahoma 74078, USA*
[72]*Brown University, Providence, Rhode Island 02912, USA*
[73]*University of Texas, Arlington, Texas 76019, USA*
[74]*Southern Methodist University, Dallas, Texas 75275, USA*
[75]*Rice University, Houston, Texas 77005, USA*
[76]*University of Virginia, Charlottesville, Virginia 22901, USA*
[77]*University of Washington, Seattle, Washington 98195, USA*

(Received 27 March 2012; published 2 October 2012)

We present the first search for new phenomena in $Z\gamma$ final states with large missing transverse energy using data corresponding to an integrated luminosity of 6.2 fb^{-1} collected with the D0 experiment in $p\bar{p}$ collisions at $\sqrt{s} = 1.96$ TeV. This signature is predicted in gauge-mediated supersymmetry-breaking models, where the lightest neutralino $\tilde{\chi}_1^0$ is the next-to-lightest supersymmetric particle and is produced in pairs, possibly through decay from heavier supersymmetric particles. The $\tilde{\chi}_1^0$ can decay either to a Z boson or a photon and an associated gravitino that escapes detection. We exclude this model at the 95% C.L. for supersymmetry-breaking scales of $\Lambda < 87$ TeV.

DOI: 10.1103/PhysRevD.86.071701 PACS numbers: 14.80.Ly, 12.60.Jv, 13.85.Rm

The production of $Z\gamma$ with large missing transverse energy in $p\bar{p}$ collisions is a rare process in the standard model (SM) and thus is an interesting experimental signature for new phenomena searches. Such a signature is predicted by well-motivated gauge-mediated supersymmetry- (SUSY-) breaking (GMSB) models [1] of physics beyond the SM. In GMSB models, SM gauge interactions serve as the messengers of SUSY breaking and thereby the masses of the SUSY partners of SM particles are connected to the strength of their gauge interactions. Assuming R-parity conservation, SUSY particles are produced in pairs, each decaying to lighter states which always include the next-to-lightest supersymmetric particle (NLSP). The final supersymmetric decay of the NLSP to SM particles and the nearly massless gravitino $\tilde{G}$ provide the typical signature used in GMSB searches.

The CDF, D0, ATLAS, CMS, and H1 Collaborations have all searched for GMSB neutralinos $\tilde{\chi}_1^0$ in the $\gamma\tilde{G} + \gamma\tilde{G}$ (and single $\gamma\tilde{G}$) final state assuming that the $\tilde{\chi}_1^0$ is the NLSP and binolike, decaying promptly to a photon and $\tilde{G}$ [2–4]. In this Letter, we present a unique search for a Higgsino-like $\tilde{\chi}_1^0$ with the $Z\tilde{G} + \gamma\tilde{G}$ final state. The GMSB model we consider is "model line E" of Ref. [5] which is characterized by six parameters: the effective SUSY-breaking scale Λ which is varied in the following, the number of sets of messenger particles which is set to $n_5 = 2$, the ratio of the Higgs vacuum expectation value which is chosen to be $\tan\beta = 3$, the mass of the messenger particles which is selected to be $M = 3\Lambda$, the Higgs sector mixing parameter μ which is taken as $\mu = (3/4)M_1$, where M_1 is the hypercharge gaugino mass, and the parameter C_{grav} which is linearly related to the gravitino mass and is set to $C_{\text{grav}} = 1$ [6]. In this model $\tilde{\chi}_1^0$ decays with substantial branching fraction to $Z\tilde{G}$, as well as to $\gamma\tilde{G}$,

---

[*] Deceased.
[†] Visitor from Augustana College, Sioux Falls, SD, USA.
[‡] Visitor from The University of Liverpool, Liverpool, United Kingdom.
[§] Visitor from UPIITA-IPN, Mexico City, Mexico.
[‖] Visitor from DESY, Hamburg, Germany.
[¶] Visitor from SLAC, Menlo Park, CA, USA.
[**] Visitor from University College London, London, United Kingdom.
[††] Visitor from Centro de Investigacion en Computacion-IPN, Mexico City, Mexico.
[‡‡] Visitor from ECFM, Universidad Autonoma de Sinaloa, Culiacán, Mexico.
[§§] Visitor from Universidade Estadual Paulista, São Paulo, Brazil.

thereby providing a promising experimental signature for the discovery of the $\tilde{\chi}_1^0$ NLSP in the $Z\tilde{G} + \gamma\tilde{G}$ final state. The gravitinos escape detection, leading to a $Z\gamma$ final state with large missing transverse energy $\not\!\!E_T$. We report a search for these events in $p\bar{p}$ collisions recorded with the D0 detector [7] at the Fermilab Tevatron Collider.

The final state for this analysis contains a Z boson decaying to e^+e^- or $\mu^+\mu^-$, a photon of large transverse energy, and large $\not\!\!E_T$. The data have been collected using a set of inclusive electron or muon triggers, corresponding to an integrated luminosity of $6.2 \pm 0.4\ \mathrm{fb}^{-1}$ [8]. The triggers have about 100% (78%) efficiency for signal in the $ee\gamma$ ($\mu\mu\gamma$) channel.

Electrons are required to have at least 90% of their energy deposited in the electromagnetic (EM) calorimeter and an EM shower distribution consistent with that expected for an electron. They are further required to be isolated in both the calorimeter and the tracker. A neural network (NN) multivariate discriminant [9], formed from the parameters of the EM shower and the track associated with the electron candidate, as well as central preshower detector information, is used to discriminate electrons from jets. For electrons with $p_T = 40$ GeV, the identification efficiency is $\approx 82\%$.

Muons are identified as track segments in the muon detector that match tracks found in the tracking system. Muons are also required to be isolated in both the calorimeter and the tracker. The identification efficiency for muons with $p_T = 40$ GeV is $\approx 79\%$.

Photons are identified in the central calorimeter and are required to be separated from leptons and jets by $\Delta R = \sqrt{(\Delta\eta)^2 + (\Delta\phi)^2} > 0.7$ [10]. Additional requirements are applied on the fraction of energy deposited in the EM calorimeter and on isolation in both the calorimeter and the tracker. The shower width in the third layer (EM3) must be consistent with that of a photon. To suppress electrons misidentified as photons, the candidates must not be spatially matched to a track or to energy depositions in the silicon microstrip or central fiber trackers that lie along the trajectory connecting the primary vertex and the calorimeter cluster [11]. Further rejection of jets is achieved with a NN discriminant similar to that used for electron selection. The average identification efficiency for photons with $p_T = 40$ GeV is $\approx 75\%$.

The $\not\!\!E_T$ is the negative of the vectorial sum of transverse components of energy depositions in the calorimeter, corrected for identified photons, electrons, and muons. Jet energies are calibrated using transverse energy balance in photon + jet and dijet events [12], and these corrections are propagated to the calculation of $\not\!\!E_T$.

To select $Z\gamma + \not\!\!E_T$ events, we first require at least two leptons. Each lepton must have $p_T > 15$ GeV, with one electron (muon) having $p_T > 25$ (20) GeV. The two leptons must have opposite charge and an invariant mass $M_{\ell\ell}$ within the Z-mass windows of 78–104 and 65–115 GeV for the ee and $\mu\mu$ channels, respectively. A total number of 261 964 (306 541) ee ($\mu\mu$) candidates satisfy these criteria. We require at least one isolated photon with $p_T^\gamma > 30$ GeV in the event. To reduce background from photons radiated by the two leptons, we require a three-body invariant mass $M(\ell\ell\gamma) > 120$ GeV, which results in a total number of 78 (91) $ee\gamma$ ($\mu\mu\gamma$) candidates. The GMSB signal is expected in the region of large $\not\!\!E_T$. We therefore require $\not\!\!E_T > 30$ (40) GeV in the electron (muon) channel. To remove events with spurious $\not\!\!E_T$ due to poorly reconstructed muons, we require that $\Delta\phi(\not\!\!E_T, \mu_1) < 2.85$, where μ_1 is the highest-p_T muon. The $\not\!\!E_T$ significance, a likelihood discriminant based on the ratio of $\not\!\!E_T$ and its uncertainty, is required to be >5. No data are selected in the $eey + \not\!\!E_T$ final state, and a single event is selected in the $\mu\mu\gamma + \not\!\!E_T$ final state.

The background to the $Z\gamma + \not\!\!E_T$ signal arises from instrumental backgrounds caused by mismeasured $\not\!\!E_T$, misidentified leptons or misidentified jets in $Z\gamma$, $Z +$ jets, WW, WZ, ZZ, $W + X$, and $t\bar{t}$ processes. The backgrounds are either estimated using control samples in data or using Monte Carlo (MC) simulated events processed using a detailed GEANT-based simulation [13] of the D0 detector response and overlaid with data from random beam crossings. The simulation is corrected for lepton identification efficiencies and energy resolutions observed in data.

The SM $Z\gamma$ process is the dominant source of background. It is estimated using PYTHIA [14]. The photon p_T spectrum from PYTHIA for initial state radiation is corrected for QCD and electroweak next-to-leading-order (NLO) effects using the MC event generator of Ref. [15]. The contribution from final state radiation is determined by fitting the $M(\ell\ell)$ distribution of $Z\gamma$ MC events to data in the range $p_T^\gamma > 10$ GeV and $\not\!\!E_T < 30$ GeV and is found to be very small because of the requirements on $\Delta R(\ell, \gamma)$, p_T^γ, $M(\ell\ell)_\gamma$ and $\not\!\!E_T$. We estimate the $Z\gamma$ contribution in the signal region to be 0.23 ± 0.05 (stat) and 0.43 ± 0.05 (stat) events in the $ee\gamma$ and $\mu\mu\gamma$ channels, respectively.

Background from $Z +$ jets events can enter the sample if a jet is misidentified as a photon and $\not\!\!E_T$ is large. Two data-driven methods are used to estimate this background. In the first method, we select an orthogonal sample of events with at least two electrons or two muons and with a jet passing all photon acceptance criteria except failing either the requirements on tracker isolation or on shower width in EM3. The $Z +$ jets background is then estimated by scaling this sample by an η-dependent factor f. This factor f is the ratio of the probability for a jet to satisfy full photon-identification criteria to the probability to fail tracker isolation or shower width requirements. It is measured using dijet data as a function of η and $\not\!\!E_T$, yielding typical values of 0.08–0.16 with uncertainties of 10%. In the second method, the $Z +$ jets background is estimated by fitting the sum of the NN templates for photons and photonlike jets to the observed photon NN distribution. Templates of

TABLE I. Cross sections σ_{p} for the production of pairs of lightest neutralinos $\tilde{\chi}_1^0$ via cascade decay, branching fractions of $\tilde{\chi}_1^0$ to $\gamma\tilde{G}$ ($\mathcal{B}_\gamma$) and to $Z\tilde{G}$ ($\mathcal{B}_Z$), and the lightest neutralino mass $M_{\tilde{\chi}_1^0}$ used in this analysis, which is parametrized by the breaking scale Λ. The $\tilde{\chi}_1^0$ also decays to Higgs + $\tilde{G}$ and to nonresonant $\ell^+\ell^-\tilde{G}$, which dominate the remaining decays for large and small Λ, respectively. Also given are the observed (expected) 95% C.L. upper limits on the production cross section using the BDT analyses.

Λ [TeV]	σ_{p} [fb]	$\mathcal{B}_\gamma$	$\mathcal{B}_Z$	$M_{\tilde{\chi}_1^0}$ [GeV]	Obs. (exp.) limit on σ_{p} [fb]
70	618	0.892	0.086	111	<234 (223)
75	419	0.715	0.253	123	<172 (150)
80	290	0.545	0.408	135	<167 (140)
85	205	0.420	0.519	147	<163 (137)
90	146	0.335	0.592	159	<186 (155)
95	106	0.277	0.642	169	<205 (159)

the NN distributions are obtained from simulations of photons and separately of jets, as the NN for data is found to be well modeled by MC [9]. The results from these two methods are consistent within their statistical uncertainties, and the first method is used since it yields smaller uncertainties. The resulting estimates of the Z + jets contribution in the signal region are 0.09 ± 0.08 (stat) and 0.17 ± 0.16 (stat) in the $ee\gamma$ and $\mu\mu\gamma$ channels, respectively.

The SM backgrounds from WW, WZ, ZZ, and $t\bar{t}$ production are estimated using MC simulations with PYTHIA [14] for dibosons and ALPGEN [16] for $t\bar{t}$. The cross sections are from MCFM [17], calculated at NLO. The $\not{E}_T$ can be substantial in such events, but none of these backgrounds are sources of isolated, high-p_T^γ photons.

The GMSB signal is modeled with the PYTHIA leading-order (LO) MC event generator using supersymmetric particle spectra calculated in ISAJET [18]. The Λ parameter is varied from 70 to 95 TeV, in steps of 5 TeV, and used to compute a minimal supersymmetric standard model particle mass spectrum and a set of branching ratios. The LO signal cross sections are scaled to match the NLO prediction from PROSPINO [19]. The inclusive cross section for the pair production of $\tilde{\chi}_1^0$ from cascade decays is 618 fb for $\Lambda = 70$ TeV and decreases to 106 fb for $\Lambda = 95$ TeV. In this model the $\tilde{\chi}_1^0$ are pair produced primarily via the weak interaction and the squarks and gluinos are pushed beyond the kinematic reach of the accelerator. The fraction of $\tilde{\chi}_1^0 \to Z\tilde{G}$ decays ($\mathcal{B}_Z$) increases with Λ, reaching 50% at $\Lambda \approx 85$ TeV. Cross sections and branching fractions are given in Table I. At larger Λ values, $Z\tilde{G}$ is the main decay mode for $\tilde{\chi}_1^0$. For the full event selection, the overall product of acceptance and efficiency of $Z(ee/\mu\mu)\tilde{G} + \gamma\tilde{G}$ events is 7.7% (5.1%) at $\Lambda = 70$ TeV and increases to 11.2% (8.6%) for $\Lambda = 95$ TeV in the $ee\gamma$ ($\mu\mu\gamma$) channel.

The expected signal yield for $\Lambda = 80$ and 90 TeV and the estimated SM backgrounds are summarized in Table II. The total background is expected to be 0.5 ± 0.1 and 0.7 ± 0.4 events in the $ee\gamma + \not{E}_T$ and $\mu\mu\gamma + \not{E}_T$ channels, respectively. The number of observed events is consistent with these expectations. The comparison between data and SM MC predictions for the $\not{E}_T$ distributions after selecting $Z\gamma$ events is given in Fig. 1 along with the signal expectation. Good agreement between data and SM background is observed for both $ee\gamma$ and $\mu\mu\gamma$ channels.

The systematic uncertainties that affect the signal and SM backgrounds include theoretical and experimental sources. The uncertainties on the theoretical cross section for diboson and $t\bar{t}$ processes are 6% and 10% [17], respectively. The uncertainty on the measured luminosity is 6.1% [8] and is applied to the SM background estimations based on MC simulation. The uncertainty on electron identification efficiency is 1% in the central calorimeter region and increases to 4% in the end-cap calorimeter. The systematic uncertainties on muon identification include 1.0% for reconstruction, 1.1% for tracking efficiency, and 0.5% for isolation. The photon-identification uncertainty is 2.7% [20]. The uncertainties from the jet energy scale are estimated to be 1% for signal and 4% for the backgrounds [12]. The uncertainty on the momentum resolution for muons is reflected in an uncertainty of ≈100% in the signal region

TABLE II. Number of observed and expected events for the restrictive criteria defining the signal region and for less stringent requirements that are followed by a selection on BDT output defining an alternative signal region. The first uncertainty is statistical and the second is systematic. The contributions from Z + jets for the BDT analyses are found to be negligible. Different $\mu\mu\gamma + \not{E}_T$ events pass the signal region selections and the BDT > 0.8 selection in data.

	$ee\gamma + \not{E}_T$		$\mu\mu\gamma + \not{E}_T$	
	Signal region	BDT > 0.8	Signal region	BDT > 0.8
Expected signal ($\Lambda = 80$ TeV)	3.28 ± 0.09 ± 0.24	3.95 ± 0.10 ± 0.50	2.42 ± 0.08 ± 0.31	2.69 ± 0.08 ± 0.33
Expected signal ($\Lambda = 90$ TeV)	1.48 ± 0.03 ± 0.11	1.73 ± 0.05 ± 0.21	1.06 ± 0.03 ± 0.14	1.22 ± 0.04 ± 0.15
$Z\gamma$	0.23 ± 0.05 ± 0.02	0.23 ± 0.11 ± 0.02	0.43 ± 0.05 ± 0.40	0.10 ± 0.03 ± 0.20
Z + jet	0.09 ± 0.08 ± 0.01	···	0.17 ± 0.16 ± 0.02	···
$WW + WZ + ZZ$	0.13 ± 0.05 ± 0.01	0.06 ± 0.04 ± 0.01	0.08 ± 0.03 ± 0.01	0.16 ± 0.19 ± 0.02
$t\bar{t}$	0.05 ± 0.01 ± 0.01	0.14 ± 0.03 ± 0.02	0.04 ± 0.01 ± 0.01	0.05 ± 0.02 ± 0.01
All backgrounds	0.50 ± 0.11 ± 0.03	0.43 ± 0.12 ± 0.03	0.71 ± 0.17 ± 0.40	0.31 ± 0.10 ± 0.20
Data	0	0	1	1

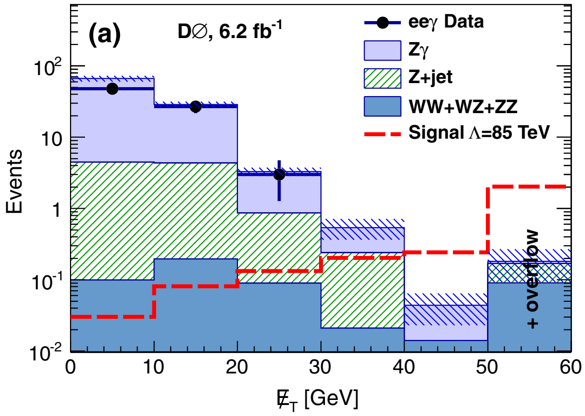

FIG. 1 (color online). Distribution of $\not\!\!E_T$ for $Z\gamma$ events in the (a) $ee\gamma$ channel and (b) $\mu\mu\gamma$ channel before requiring $\not\!\!E_T$ significance >5. The hatching on the sum of background contributions indicates the total uncertainty on the background prediction.

$\not\!\!E_T > 40$ GeV on the estimate of the background from $Z(\mu\mu) + \gamma$.

To improve the sensitivity for $\tilde{\chi}_1^0$ detection at the cost of a stronger dependence on the specifics of the GMSB model, we also use a boosted decision tree (BDT) multivariate technique to discriminate between SM background and signal [21]. The output is a discriminant that is shifted toward $+1$ for signal and strongly peaked near -1 for background events.

The BDT is trained on a randomly selected collection of signal and background MC events, Z + jet background candidates from data, and a signal assuming $\Lambda = 90$ TeV. The training samples require a leading lepton of $p_T > 25(20)$ GeV, a second lepton of $p_T > 15$ GeV, $p_T^\gamma > 20$ GeV, $M(\ell\ell\gamma) > 120$ GeV, $\not\!\!E_T > 15$ GeV and $M(\ell\ell) > 70(65)$ GeV in the $ee\gamma$ ($\mu\mu\gamma$) channel. A set of 14 sensitive variables, well modeled by the simulation, is used to form the BDT discriminant. The variables include transverse momenta of the two leptons, photon, dilepton system, and dilepton + photon system, as well as $\not\!\!E_T$ and $M(\ell\ell\gamma)$. The expected signal and background yields are estimated from events independent of the set used for training. The data are found consistent with the SM background prediction as seen in Fig. 2 and Table II (for BDT >0.8), and no evidence is observed for a GMSB neutralino NLSP.

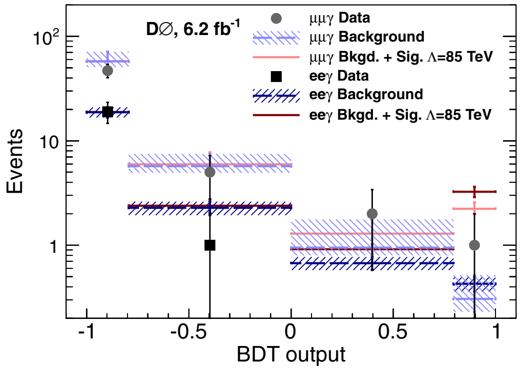

FIG. 2 (color online). Distribution of BDT output in the $ee\gamma$ channel and $\mu\mu\gamma$ channel for background only, background with a $\Lambda = 85$ TeV signal added, and data. The total background uncertainties are indicated as shaded bands.

Limits on the production cross section of $\tilde{\chi}_1^0\tilde{\chi}_1^0$ using the benchmark model are derived using a Poisson log-likelihood ratio as test statistic, combining results from the electron and muon channels. Pseudoexperiments are generated according to the background-only and signal + background hypotheses, and systematic uncertainties are accounted for by integrating over uncertainties parametrized as Gaussian. The limits on cross sections are evaluated using the modified frequentist approach [22]. Data and background estimates are studied in four bins of BDT output, and values from the most signal-like bin (BDT $>$ 0.8) are shown in Table II. The 95% C.L. upper limit on the cross section using the BDT discriminant is shown in Fig. 3, together with the expected limit and the 1 and 2 standard deviation uncertainty bands. The 95% C.L. limits

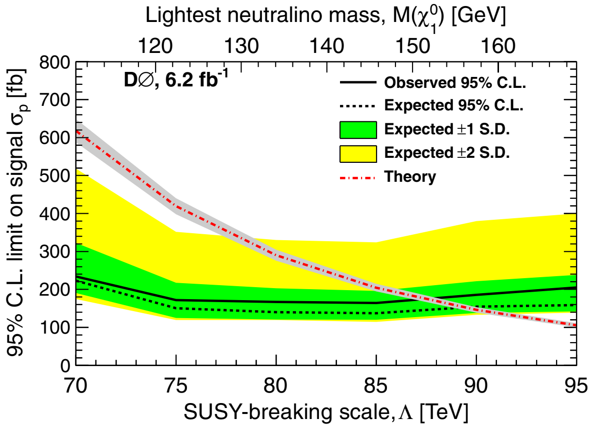

FIG. 3 (color online). Limit on the cross section for $Z\gamma + \not\!\!E_T$ production as a function of Λ (lower horizontal axis) and $M(\tilde{\chi}_1^0)$ (upper horizontal axis) at 95% C.L. combined for the $ee\gamma$ and $\mu\mu\gamma$ channels. The NLO cross section for the signal, with a band indicating the parton distribution function uncertainty, is overlaid.

on σ_p are also given in Table I. The GMSB parameters were chosen to have significant branching of $\tilde{\chi}_1^0$ to $Z\tilde{G}$ as already described. Fixing all parameters except Λ, we exclude $\Lambda < 87$ TeV at 95% C.L. using the BDT selection, which increases the expected exclusion in Λ by 4 TeV in comparison to the analysis performed without using the BDT requirement.

In summary, we present the first search for a SUSY signature in events containing $Z\gamma + \not{E}_T$ final states using 6.2 fb^{-1} of integrated luminosity collected by the D0 experiment in $p\bar{p}$ collisions at $\sqrt{s} = 1.96$ TeV. The signature corresponds to a GMSB model where pairs of neutralino NLSPs are either produced promptly or from decays of other supersymmetric particles in $p\bar{p}$ collisions and then decay to either $Z\tilde{G}$ or $\gamma\tilde{G}$. In the signal region we observe no event in the $ee\gamma$ and one event in the $\mu\mu\gamma$ channels, where the SM background is expected to be 1.21 ± 0.45 combined. Employing a multivariate selection process and combining the results from both channels, the specific neutralino NLSP model is excluded at the 95% C.L. for $\Lambda < 87$ TeV. Because of the sizable branching fraction of $\tilde{\chi}_1^0 \to \gamma\tilde{G}$ in our model, recent searches in the $\gamma\gamma + \not{E}_T$ final states [2] at the Tevatron can be expected to have comparable sensitivities, but no searches have been carried out considering the unique, Higgsino-like $\tilde{\chi}_1^0$ model examined here.

We thank the staffs at Fermilab and collaborating institutions, and acknowledge support from the DOE and NSF (USA); CEA and CNRS/IN2P3 (France); MON, Rosatom and RFBR (Russia); CNPq, FAPERJ, FAPESP and FUNDUNESP (Brazil); DAE and DST (India); Colciencias (Colombia); CONACyT (Mexico); NRF (Korea); FOM (Netherlands); STFC and the Royal Society (United Kingdom); MSMT and GACR (Czech Republic); BMBF and DFG (Germany); SFI (Ireland); The Swedish Research Council (Sweden); and CAS and CNSF (China).

---

[1] M. Dine and A. E. Nelson, Phys. Rev. D **48**, 1277 (1993); M. Dine, A. E. Nelson, and Y. Shirman, Phys. Rev. D **51**, 1362 (1995); M. Dine, A. E. Nelson, Y. Nir, and Y. Shirman, Phys. Rev. D **53**, 2658 (1996); for a review see G. F. Giudice and R. Rattazzi, Phys. Rep. **322**, 419 (1999).

[2] D. E. Acosta *et al.* (CDF Collaboration), Phys. Rev. D **71**, 031104 (2005); T. Aaltonen *et al.* (CDF Collaboration), Phys. Rev. Lett. **104**, 011801 (2010); V. M. Abazov *et al.* (D0 Collaboration), Phys. Rev. Lett. **94**, 041801 (2005); Phys. Lett. B **659**, 856 (2008); Phys. Rev. Lett. **105**, 221802 (2010).

[3] CMS Collaboration, Phys. Rev. Lett. **106**, 211802 (2011); ATLAS Collaboration, Phys. Lett. B **710**, 519 (2012).

[4] A. Aktas *et al.* (H1 Collaboration), Phys. Lett. B **616**, 31 (2005).

[5] H. Baer, P. G. Mercadante, X. Tata, and Y. Wang, Phys. Rev. D **62**, 095007 (2000).

[6] H. Baer, P. G. Mercadante, F. Paige, X. Tata, and Y. Wang, Phys. Lett. B **435**, 109 (1998).

[7] V. M. Abazov *et al.* (D0 Collaboration), Nucl. Instrum. Methods Phys. Res., Sect. A **565**, 463 (2006); M. Abolins *et al.*, Nucl. Instrum. Methods Phys. Res., Sect. A **584**, 75 (2008); R. Angstadt *et al.*, Nucl. Instrum. Methods Phys. Res., Sect. A **622**, 298 (2010).

[8] T. Andeen *et al.*, Report No. FERMILAB-TM-2365, 2007.

[9] V. M. Abazov *et al.* (D0 Collaboration), Phys. Rev. Lett. **102**, 231801 (2009); Phys. Lett. B **690**, 108 (2010).

[10] The polar angle θ, the azimuthal angle ϕ, and transverse quantities such as transverse momentum p_T are defined with respect to the z axis, which is along the proton beam direction, and the center of the D0 detector. Pseudorapidity is defined as $\eta = -\ln[\tan(\theta/2)]$.

[11] V. M. Abazov *et al.* (D0 Collaboration), Phys. Lett. B **659**, 856 (2008).

[12] V. M. Abazov *et al.* (D0 Collaboration), Phys. Rev. Lett. **101**, 062001 (2008); Phys. Rev. D **85**, 052006 (2012).

[13] R. Brun and F. Carminati, CERN Program Library Long Writeup W5013, 1993; we use GEANT version v3.21.

[14] T. Sjöstrand, S. Mrenna, and P. Skands, J. High Energy Phys. 05 (2006) 026.

[15] V. Barger, T. Han, D. Zeppenfeld, and J. Ohnemus, Phys. Rev. D **41**, 2782 (1990); U. Baur, T. Han, and J. Ohnemus, Phys. Rev. D **48**, 5140 (1993); J. Ohnemus, Phys. Rev. D **51**, 1068 (1995).

[16] M. L. Mangano, F. Piccinini, A. D. Polosa, M. Moretti, and R. Pittau, J. High Energy Phys. 07 (2003) 001. Version 2.11 was used.

[17] N. Kidonakis and R. Vogt, Phys. Rev. D **78**, 074005 (2008); J. M. Campbell and R. K. Ellis, Phys. Rev. D **60**, 113006 (1999).

[18] H. Baer, F. E. Paige, S. D. Protopescu, and X. Tata, arXiv:hep-ph/0312045.

[19] W. Beenakker, M. Klasen, M. Krämer, T. Plehn, M. Spira, and P. Zerwas, Phys. Rev. Lett. **83**, 3780 (1999).

[20] V. M. Abazov *et al.* (D0 Collaboration), Phys. Rev. D **85**, 052001 (2012).

[21] B. P. Roe, H.-J. Yang, J. Zhu, Y. Liu, I. Stancu, and G. McGregor, Nucl. Instrum. Methods Phys. Res., Sect. A **543**, 577 (2005); H.-J. Yang, T. Dai, A. Wilson, Z. Zhao, and B. Zhou, JINST **3**, P04004 (2008).

[22] T. Junk, Nucl. Instrum. Methods Phys. Res., Sect. A **434**, 435 (1999); A. Read, J. Phys. G **28**, 2693 (2002); W. Fisher, Report No. FERMILAB-TM-2386-E, 2006.